E JOURNAL

3D-Printing on medical textiles – Investigation of adhesion and interpenetration of extruded polymers on knitted PET fabric substrate

Marius Meyer (M. Sc.) [a], Lars Meyer (M. Sc.) [a,b], Dr.-Ing. Stefan Kleszczynski [a,c]

[a] Universität Duisburg-Essen, Lehrstuhl für Fertigungstechnik,
Lotharstr. 1, 47057 Duisburg, Deutschland

[b] AM Filament GmbH, Elbinger Weg 8, 45470 Mülheim an der Ruhr, Deutschland

[c] CENIDE, Center for Nanointegration Duisburg-Essen,
Carl-Benz-Str. 199, 47057 Duisburg, Deutschland

https://doi.org/10.58134/fh-aachen-rte_2024_015

Zusammenfassung Dieses Paper untersucht den Einfluss der Extrusionstemperatur bei der additiven Fertigung mit dem Materialextrusionsverfahren (MEX) auf das Adhäsionsverhalten bei der Fertigung auf einem Substrat aus Synthetikfasern aus Polyethylenterephthalat (PET), das für den Einsatz in textilbasierten medizinischen Implantaten entwickelt wurde. Zusätzlich zur Adhäsion des extrudierten Filaments auf dem Substrat wird auch dessen Fähigkeit zur Bildung einer formschlüssigen Verbindung durch Interpenetration, also der Durchdringung des Gewebes, untersucht. Zur Vergleichbarkeit der Ergebnisse wird die Verbindung zwischen Substrat und Extrudat mittels Zugversuchs geprüft. Als Teil dieser Untersuchung wurden mehrere Versuchsreihen mit eigens gefertigten Probenkörpern aus einem herkömmlichen Polylactid (PLA) und zwei verschiedenen Polyamiden (PA12) durchgeführt. Somit können nicht nur die Testreihen untereinander hinsichtlich ihrer Extrusionsparameter verglichen werden, sondern die Ergebnisse tendenziell auch auf weitere Polymere bzw. Filamente übertragen werden.

Abstract This work investigates the influence of the extrusion temperature used in material extrusion (MEX) additive manufacturing (AM) on the holding strength of parts fabricated onto a synthetic fiber knitted fabric made of polyethylene terephthalate (PET), which was developed for use in textile implants for medical applications. In addition to the adhesion of the extruded filament to the substrate, its ability to create a form-fit bond by interpenetration, i.e. infiltration of the textile, is also investigated. To compare results, the bond between the substrate and extrudate is then examined using a tensile test. As part of this investigation, several series of tests were conducted on samples made from a polylactide (PLA) and two different polyamide 12 (PA 12) filaments. In addition to being able to compare individual test series based on the results and associated extrusion parameters, the results can also be transferred to other polymers and/or filaments.

Keywords additive manufacturing, material extrusion, medical application, interpenetration, composite material, extrusion temperature

Introduction

Research over the past two decades has led to the continuous evolution of common AM processes. While powder bed fusion processes (PBF-LB/M for metals and PBF-LB/P for plastics) require expensive systems and peripherals, and stereolithography (SLA) is more complex to handle due to the use of liquid photopolymers, MEX has become more and more established, particularly in the private sector. This is due to lower cost structures and generally shorter production times for the same components in comparison to other AM processes [1]. The functionality of MEX also allows to process different materials within one printing process, which opens a wide range of possibilities in the field of composite materials and components [2–4].

While the use of composite materials in the form of filaments (e.g. glass- or carbon-fiber-filled) is already established, the production of components from different filaments is usually limited to chemically similar or even identical filaments, usually with the aim of creating multicolored (decorative) components [4–6]. MEX systems with two extrusion tools, one of which is solely dedicated to the creation of support structures (e.g. water-soluble polyvinyl alcohols), are also common [7]. As support structures are only needed during manufacturing and are removed afterwards, this process generally does not produce composite parts. The production of such components is mainly used in the technical field to create a synergy between several materials, e.g. in the production of functional surfaces in plain bearings [4]. Other applications of MEX processes in the field of composites, such as the incorporation of support structures into aramid-based textiles or the designing of smart clothing, are mainly carried out in research done in universities (e.g. Polytechnic University Hong Kong, China, Polytechnic University of Tirana, Albania, or Bielefeld University of Applied Sciences, Germany) [8–11]. Other processes that use liquid materials (such as material jetting or liquid deposition) also have the potential for being used with textiles. However, because of their mechanical properties, these parts are typically used in decoration or in fields, where a certain deformation is necessary, i.e. sealing [8, 12].

Another field in which the processes mentioned can be of great benefit is the manufacturing of individualized medical products like implants or prosthetics. For example, joint replacements or drug-eluting implants, which are implants that release medication on an ongoing basis, are already being produced using AM [13, 14]. Additionally, many medical products rely on textile structures, mostly due to the flexibility of textiles when compared to solid polymer components [15]. To date, however, there has been no systematic investigation of how MEX structures adhere to medically certified PET textiles. This work aims to close this gap by determining the parameters needed to combine both compounds. Due to the high requirements in this field, especially in terms of biocompatibility, only a few polymers can be considered for this purpose, as in addition to the base material, each additive must also be tested for its medical suitability [16]. This also limits the choice of manufacturing process, as SLA components, for example, are made from liquid resins that are potentially hazardous to health in their original state and can exhibit measurable toxicity after processing [17]. A potentially restricting factor of powder bed fusion processes is the regulation of nanoparticles, which appears to be negligible due to the average particle size in the powder [16, 18]. However, the enclosed and heated installation space of such systems makes it considerably more difficult to realize major adjustments within the manufacturing process, such as the required insertion of the substrate textile. In order to close this supply gap in the AM processes, the possibilities offered by the MEX process must be explored.

Methods and Materials

Due to the multitude of variable parameters in AM processes, care must be taken to keep the possible influences on the process as small and controllable as possible. In addition to the equipment and materials used in the process, the manufacturing and test parameters in particular should be mentioned here in order to ensure comparability with already existing literature and future studies.

Printer and nozzle

All samples were produced on a modified *E3D toolchanger* equipped with a water-cooled, high-temperature hot end (*Mosquito Liquid, Slice Engineering*) with a 0.4 mm nozzle diameter to be able to use filaments with processing temperatures above 300 °C. Although the pre-installed hot end allows the processing of most filaments used in the conducted experiments, it is crucial to keep as many parameters as possible identical for comparability. As different hot ends can have varying (and usually empirically determined) operating points and offsets, the high-temperature hot end is also used for polymers with lower processing temperatures to ensure comparability of results with future high-temperature polymer measurement series, in addition to enabling a raise of the extrusion temperature for one of the materials used in the conducted experiments. The heated bed will not be used as introducing further heat into the production process could result in an increased risk of damaging the substrate material. For the same reason, the entire fabrication process is carried out with maximum part cooling so that excess heat can be dissipated more quickly after the extrudate is bonded to the substrate.

Materials and processing temperatures

Due to the strong influence of fiber reinforcement on mechanical behavior and also a possible alteration of adhesive properties due to those fibers, only unfilled thermoplastic polymers are used. Where possible, colored filaments are used for better visual inspection of the bonding result, however one of the materials used in the experiments is only available uncolored. A possible influence of coloring additives is estimated as negligible or non-existent. In addition to a conventional PLA filament (*PLA Extrafill Orange* by *Fillamentum Manufacturing Czech s.r.o., Hulin, Czech Republic*), two PA12 filaments will be investigated, one of which is already being used for further material investigations in the medical field and has been optimized for this application in terms of its processing temperature. To differentiate between these two filaments, the optimized filament (*MeltFox PA12 Polar Bear White* by *AM Filament GmbH, Mülheim an der Ruhr, Germany*) is given the suffix "LT" (low temperature) and the standard filament (*ePA12 black* by *Shenzhen Esun Industrial Co., Shenzhen, China*) the suffix "HT" (high temperature). For a complete list of tested temperatures, see ***Table 1***.

Table 1 - Materials and processing temperatures

Material	T1 in °C	T2 in °C
PLA	210	230
PA12HT	290	310
PA12LT	250	270

As the aim of these experiments is to evaluate the general adhesion and interpenetration mechanisms within this purpose, it was decided to not use PET-G filament, as this polymer was expected to create a bond not only through adhesion, but also through merging due

to being chemically related to the substrate material. The decision on the three polymers was based on their availability (PLA), being developed for this use case (PA12LT) and comparability between specialized and regular filaments of the same type (PA12HT).

Based on prior testing with PLA and previous findings, the filament manufacturer's upper processing temperature was selected as the first temperature to investigate. In the second tests, this temperature was exceeded by another 20 °C. In all cases, the second processing temperature is already in the range of the first thermal decomposition mechanisms, but still below complete pyrolysis. [9, 10, 19–21]

Sample geometry and manufacturing

The test samples consist of a thin sheet of material extruded onto the (approximately 0.1 mm thick) PET textile substrate. The extruded panel itself is 0.5 mm thick, 30 mm in length and 5 mm in width. Since the primary objective is to test the bond between the material and the textile, the samples have a remainder of unaltered substrate on one side and an overhang of the extruded material on the other side. This results in a intended breaking point (***Fig. 1***), which allows to characterize the bonding between the joint surfaces by performing tensile tests. During the testing both the substrate and the extruded material are clamped (as in ***Fig. 3***) and peeled off in a controlled manner by applying a tensile force.

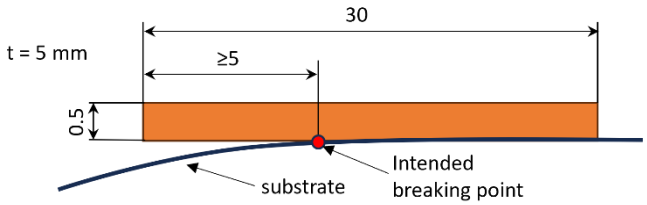

Fig. 1 – sample structure

The test samples are printed directly onto (and partially into) the substrate with an initial layer height of 0.3 mm and then stabilized with a second, regular layer with a height of 0.2 mm. These layers were applied with default shell and infill parameters within *SuperSlicer* (3 perimeters and a solid infill in a 45-degree angle) as these settings are commonly used as default in most slicing softwares. To ensure penetration of the first layer of material, it is necessary to reduce the distance between the nozzle and the substrate, since by default the amount of material extruded fills exactly the volume between the nozzle and building surface. As the volume to be filled is partly within the substrate, the nozzle distance has been reduced by half the layer height. This equates to a z-offset equal to -0.15 mm (or -0.1 mm for the 290 °C and 310 °C test series) in relation to the nozzle distance needed for optimal adhesion on a regular heated bed [20]. The slight increase in distance for the higher temperature measurement series was necessary to prevent the substrate material from being destroyed due to the increased heat exposure.

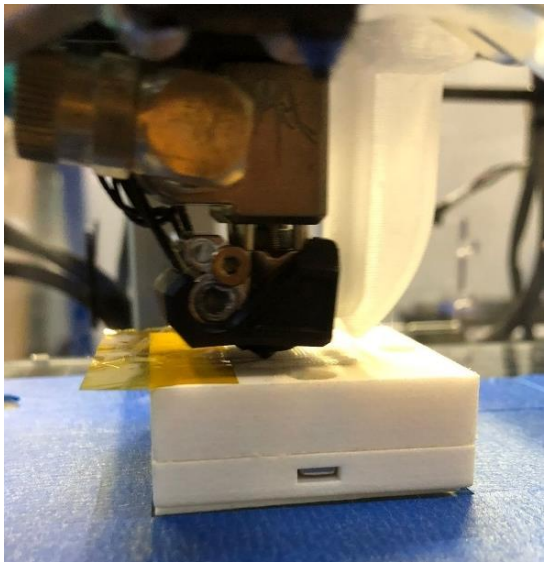

Fig. 2 - Production of a sample in the fixture

To fabricate the samples, a fixture (***Fig. 2)*** was developed, into which the textile can be clamped to counteract any movement of the material caused by the movement of the hot end. A polyetherimide (PEI) adhesive tape, which is also used in conventional heated beds, due to its surface properties and temperature resistance, was applied to realize the material overhang and ensure a non-destructive removal of the sample.

Testing

The bond between the textile and the extruded material was tested using a uniaxial universal testing machine (*Shimadzu AGS-X 10 kN*). The test speed was 100 mm/min with a time resolution of 0.01 seconds with a measurement resolution of ±1 % between 20 N and 10 kN [22]. Once a complete drop in force was registered within a single measurement step, the sample was considered destroyed, indicating either a tear in the fabric or a complete separation of the bond.

The samples were clamped into the testing machine as shown in ***Fig. 3*** to simulate the most unfavorable load case for the present application. The axial traveling distance and possible elongation of the samples themselves are not part of the tests, so no pre-stretching of the samples was performed. Evaluation of the measurement series includes consideration of the force curves and maximum forces as well as the failure mechanism of each sample.

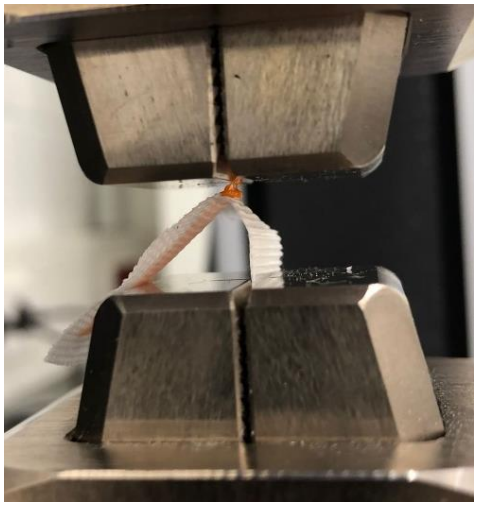

Fig. 3 - Clamping of the sample

In total, the tensile tests consist of six test series (two for each material, one each for T1 and T2 as shown in ***Table 1***). Five samples were prepared for each test series in order to obtain statistically significant results. In both series of tests with PLA, as well as the series of tests with PA12HT at 290 °C, only four samples were tested due to manufacturing errors (i.e. damaged textile due to the nozzle getting too close). The tests are not evaluated in accordance with ISO 527, as these are adapted test samples specifically designed for this use case.

Results and evaluation

A comparison of stress and strain is not possible because it requires a determinable cross-section of the bond, which in turn would have to be determined by the shape and quality of the bond itself. This is finally part of the investigations performed here and might be considered for future work. In addition, due to the composite nature of the material, it is not possible to clearly assign what portion of the elongation is attributable to which material. Since the fracture behavior of the samples cannot be accurately predicted, all tests are evaluated regardless of whether they resulted in the bond being completely broken or the substrate being torn.

Therefore, the analysis is based solely on the measured forces and the visible failure mechanisms of the samples. For this purpose, the maximum forces determined for each sample are read out and displayed in the form of a dot plot. The damage pattern of each sample is used to determine the extent to which the substrate or extruded geometry was damaged when the bond came undone.

Forces

When considering the forces, it is important to note that these are only the maximum values measured during the entire test procedure. Since the samples do not exhibit isotropic material behavior, it is not possible to explicitly assign these values at the local level. The force values are subject to large fluctuations of, in some cases, more than 50 % between local maxima over the course of the measurement. This means that the failure mechanism is not continuous, and therefore the individual bonds within a single sample will have different holding forces. These differences were not in the scope of the investigations and will be part of future work. Manual evaluation also revealed no

detectable correlation between the location and magnitude of the fluctuations and the extrusion temperature used for each sample. In addition to this, the bond was also not fully broken in all samples during the tensile tests, as the test automatically stops after detecting a complete drop in force, even if the bond is still partially intact. In view of the unknown influence of the test procedure on the material behavior, the affected samples were only tested once and have not been re-tested, if there was no complete separation.

As can be seen in ***Fig. 4***, the series of measurements with the lowest processing temperature of 210 °C (PLA-210) has both the lowest force and the smallest scatter, with an average holding force of 3.78 N and a standard deviation of 0.076 N. By increasing the extrusion temperature to 230 °C (PLA-230), the average holding force was increased to 5.42 N with a slightly larger standard deviation of 0.92 N. PA12HT shows a similar trend, but with a significantly greater jump in the measured holding forces between the two processing temperatures. While an average holding force of 4.62 N with a standard deviation of 0.66 N is achieved at the lower temperature of 290 °C (PA12HT-290), the average value at 310 °C (PA12HT-310) is 8.94 N with a standard deviation of 3.83 N. The application-optimized PA12LT also shows a significant difference in the holding force of the two measurement series, however the scatter is almost identical between both temperatures, contrary to the results of the other two filaments used. The average holding force at the lower extrusion temperature of 250 °C (PA12LT-250) is 15.83 N with a standard deviation of 2.11 N, and at the higher temperature of 270 °C (PA12LT-270) is 16.69 N and 2.01 N, respectively.

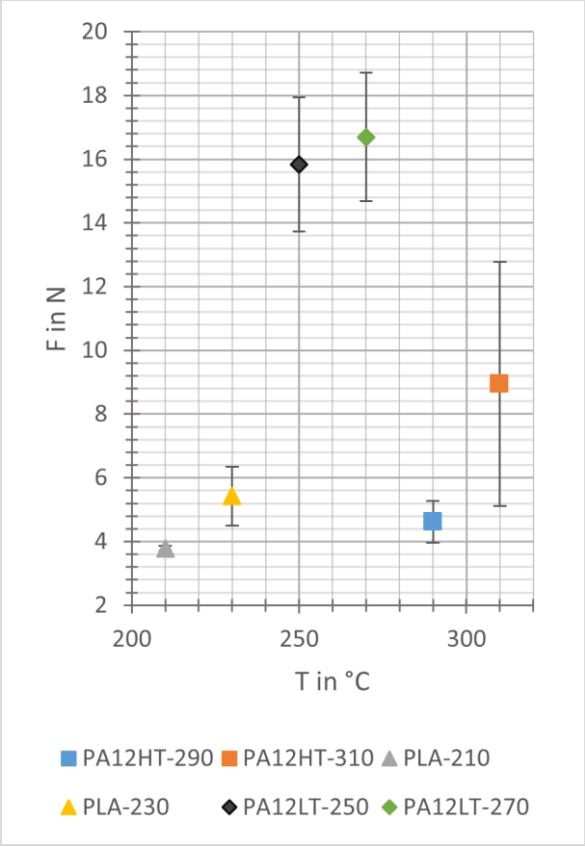

Fig. 4 – Display of mean maximum forces and standard deviations for the maximum holding forces of all measurement series

For all three filaments used, the mean value of the force required to separate (or break) the bond is higher in the second set of measurements, where extrusion was carried out at an increased temperature. In particular, the holding forces of PLA-230, PA12HT-310 and both series with PA12LT are subject to considerable fluctuations of more than 20 % around the mean value. While an increase in temperature tends to be associated with an increase in holding force, exceeding a certain limit will most-likely result in increased scattering, possibly due to the equally increasing heat flow. This limit seems to depend not only on the substrate material, but also on the extrudate material, as the results of the two series of measurements for PA12LT are very close to each other, while the results for PA12HT, despite significantly higher extrusion temperatures, show large differences. The same tendency is observed on to the two series of samples made from PLA. For both PA12HT and PLA, it is noticeable that the measurement series with a lower temperature shows less scattering than the respective measurement series with a higher temperature. This indicates that the materials in these series bond only through adhesion and not through form fit and interpenetration. These observations also suggest a link between an increased extrusion temperature and an increase in interpenetration or form fit.

Failure mechanisms

The failure mechanism of the samples can be roughly divided into three cases, which in turn will be assigned to the respective samples during the examination. Since there was no breaking of the extruded sheet in any of the tests, this classification is entirely based on the damage pattern of the textile substrate. A distinction is made between separation of the sheet from the substrate without damage (Type 1), with slight damage or remaining extrudate on the substrate (Type 2), or complete destruction of the textile (Type 3). If the bond has not been completely removed, only the separated parts will be considered for classification. This evaluation is done visually and based on the images displayed in ***Fig. 5*** (For IP protection reasons, the visible textile structure, apart from local damage, has been made unrecognizable). The samples PLA-210-5, PLA-230-1 and PA12HT-290-1 were not tested due to errors during manufacturing and are therefore not considered.

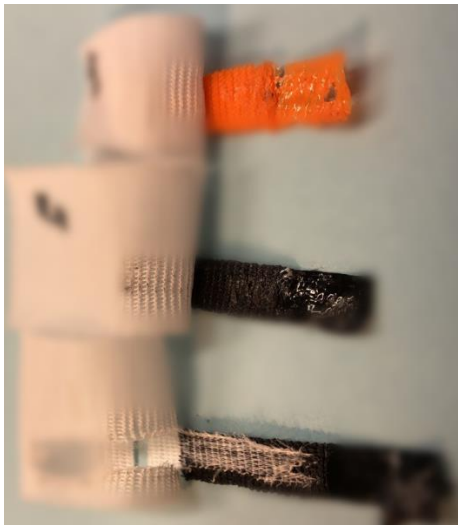

Fig. 5 – Classification of damage from top to bottom:
Type 1 (PLA-230-3), Type 2 (PA12HT-290-4),
Type 3 (PA12HT-310-1)

Many of the samples cannot be clearly assigned to one of the cases at first glance. For distinction between types 1 and 2, the samples were examined on whether the textiles showed local damage, deformation or residual extrudate in addition to overcoming the bond's adhesion, in which case they were assigned to type 2. The distinction between type 2 and type 3 is based on whether the damage is sporadic or extensive, i.e. along the entire bonding surface. Single deformations are classified as type 2, visible tears in the textile exceeding > 1 mm in length are classified as type 3.

As seen in ***Table 2***, the failure mechanisms of each series of measurements differ significantly. While the measurement series for PLA show no visible damage, the degree of damage increases with increasing extrusion temperature. In the PA12HT-290 and PA12LT-250 test series, small deformations and displacements in the textile can be seen, while there are still so visible tears. In the PA12HT-310 and PA12LT-270 test series, several samples showed significant tears in the substrate as a result of tensile testing. Additionally, sample PA12HT-290-1, which could not be tested due to damage caused by insufficient nozzle distance during production, also shows damage that can be classified as type 3.

Table 2 – Failure mechanisms of all samples

series / sample no.	1	2	3	4	5
PLA-210					
PLA-230					
PA12LT-250					
PA12LT-270					
PA12HT-290					
PA12HT-310					

Type 1 Type 2 Type 3

From the lack of substrate damage in the PLA measurement series, it can be concluded that there was no significant interpenetration in any of the samples. At the higher processing temperature of the PLA-230 series, the material tended to penetrate deeper into the substrate, as evidenced by the stronger imprint of the textile structure at the bonding surface. The samples made from PA12 show greater penetration of the textile structure for both filaments in the series of measurements with a higher extrusion temperature (PA12HT-310 and PA12LT-270) and consequently greater damage (type 3) in half of the samples. The samples from the PA12HT-290 series, in which the extrusion temperature is between the temperatures of the two previously mentioned series, show less damage in comparison, indicating poorer penetration. Test series PA12LT-250 shows a similar damage pattern, whereby the damage to the substrate is more extensive than that of test series PA12HT-290. This indicates stronger penetration (and thus interpenetration of extrudate and substrate) despite the lower processing temperature and the bond is held not only by adhesion, but mainly by form fit. The conclusions drawn from the damage patterns in the samples are consistent with the assumptions based on observation of the holding forces measured in the previous chapter and confirm the thesis of interpenetration, and hence form fit, being significantly dependent on extrusion temperature.

Conclusion

The measured holding forces and the observed damage to the substrate after separating the extruded sheet from the substrate allow clear conclusions to be drawn about the material and component behavior. For all three materials analyzed, higher extrusion temperatures generally result in a stronger bond between the two material systems. This is consistent with other research in this field, which investigated the basic mechanism of additive manufacturing on textile substrates. Contrary to the tests carried out in this paper, the used substrate materials were not knitted fabrics made of synthetic fibers, but various cotton textiles, both woven and knitted, which have a significantly lower sensitivity to heat [19]. As a result, further challenges arise during the production of the sample bodies. In addition to sufficient material penetration of the extrudate, the heat supply must also be considered to not damage the substrate and thereby reduce the strength of the bond. [9, 20]

Furthermore, a higher temperature of a polymer melt leads to a lower viscosity (when below pyrolysis) and opens up the possibility of penetrating the gaps in the textile [23]. Based on the series of tests performed here, this explains the increase in adhesion and interpenetration of the samples manufactured with a higher extrusion temperature for all used filaments. This is also confirmed by the damage patterns of each individual measurement series, as, regardless of the actual force values achieved, all measurement series with increased extrusion temperature tend to show a stronger bond and greater damage after separation. Even in the measurement series on PLA, where there was no visible damage to the substrate, there was clear evidence of improved penetration into the substrate in the samples with higher extrusion temperatures, as the textile structure left deeper impressions in the extruded sheets. In addition to a reduced viscosity of the same polymer melt at a higher temperature, this behavior can also be explained by comparing the MFI (melt flow index, in g/10min) of all three materials used. While the data sheets show a large difference between PLA (MFI 6 g/10 min at 210 °C and 2.16 kg) and PA12HT (MFI 55.64 g/10 min at 270 °C and 2.16 kg), measurements for PA12LT showed even higher flow rates (MFI 113.05 g/10 min at 250 °C and 2.16 kg) [24, 25]. These flow rates also explain the lower holding forces while showing similar damage patterns in the PA12HT test series compared to the PA12LT test series, as both materials appear to be able to penetrate deeply into the fabric, while the higher extrusion temperature of PA12HT results in a greater heat exposure, leading to a structural weakening of the substrate. Additionally, even though the MFI of PA12HT is almost ten times greater than the MFI of PLA, any benefit regarding the interpenetration is negated by the difference in process temperature, as the increased heat significantly damages the textile, which results in similar holding forces for both materials. This is particularly reflected in the large scatter of the values for the PA12HT-310 measurement series. The PA12LT material, which has been optimized in regard to its processing temperature, shows a clear interpenetration, but also paired with a similarly high scatter in both series of measurements, which suggests that the penetration of the textile simultaneously implies both a stronger bond and a higher risk of heat-related material damage. As a result, there is a realistic processing window with two limitations: a lack of bonding strength and the destruction of the textile substrate. The bond between the extruded component and the substrate is considered to be optimal when a sufficiently high holding force is achieved through form fit or interpenetration with minimal damage to the substrate. As a point of reference, a damage pattern between type 2 and type 3 in ***Fig. 5*** seems the most reasonable to guarantee structural integrity in this application, while also trying to maintain a preferably low processing temperature of 250

– 270 °C for this substrate. As higher temperatures might result in a similar damage pattern, but reduced bonding strength, it is crucial to take into account both damage pattern and maximum holding forces.

Outlook on future work

The tendencies shown here are most likely to be applicable to other thermoplastics due to the fundamentally similar material behavior of thermoplastic polymers when exposed to heat [23]. At the same time, it becomes evident that this process is based on a two-material system in which an optimized processing point must be determined iteratively for each individual filament, ensuring maximum interpenetration while minimizing heat damage to the substrate. This in turn means that each possible material combination of substrate and extrudate requires its own preliminary testing to determine this processing point. These tests should include extrusion temperature, nozzle distance, cooling, extrusion rate and speed, as these are the main parameters influencing the heat input.

The evaluations up to this point open up a wide range of possibilities for further investigations in this area. Besides directly comparing individual polymers or polymer blends, it is possible to investigate the extent to which the processing window can be extended by adjusting other boundary conditions. In addition to the selection of substrate materials with similar or even higher continuous operating temperatures than the printed filament, it is also conceivable that the viscosity could be influenced by using specific additives to ensure a low viscosity melt and thus high interpenetration even at lower processing temperatures. [26]

Regarding the intended use of the substrate presented here as part of medical implants, it appears reasonable to select the aforementioned processing point based on the highest possible holding force, since the effects of material separation could be much more severe than minor damage to the textile. The required durability of such implants is several years and requires a fatigue strength that, according to the results of the tests performed here, is more likely to be achieved by interpenetration than by adhesion.

The samples used here are relatively small compared to standard test samples (according to ISO 527) and were designed at the beginning of the test planning to produce as many samples with different parameters as possible due to the small amount of substrate material in stock. Although the samples are sufficient for the investigations carried out here, for further research, especially for larger series of tests on optimal processing points, it would be useful to develop more stable samples and possibly also individual testing devices in order to ensure comparability of the results. [9]

Acknowledgement

All product and brand names mentioned may be registered trademarks of the manufacturer, even if they are not explicitly marked as such. Special thanks go to PerAGraft GmbH for providing the textile material that was used as a substrate for the samples, AM Filament for its support in using the optimized PA12 filament, and the Chair of Engineering Design and Plastics Machinery at the University of Duisburg-Essen for its support in carrying out the tensile tests.

This work is part of a collaborative research project by the German Federal Ministry of Education and Research (*BMBF-Verbundprojekt 13GW0608E*).

Contributions

Conceptualization, methodology, formal analysis and investigation, writing – original draft preparation: Marius Meyer; **Writing - review and editing:** Marius Meyer, Lars Meyer and Stefan Kleszczynski; **Resources and supervision:** Lars Meyer and Stefan Kleszczynski

Contact details

Marius Meyer (corresponding author)
Lotharstr. 1, 47057 Duisburg)
E-Mail: marius.meyer@uni-due.de
WEB: www.uni-due.de/fertigungstechnik/

References

[1] C. M. Choudhari and V. D. Patil, "Product Development and its Comparative Analysis by SLA, SLS and FDM Rapid Prototyping Processes," *IOP Conf. Ser.: Mater. Sci. Eng.*, vol. 149, p. 12009, 2016, doi: 10.1088/1757-899X/149/1/012009.

[2] R. S. Araujo, C. R. Silva, S. P. N. Netto, E. Morya, and F. L. Brasil, "Development of a Low-Cost EEG-Controlled Hand Exoskeleton 3D Printed on Textiles," *Frontiers in neuroscience*, vol. 15, p. 661569, 2021, doi: 10.3389/fnins.2021.661569.

[3] M. L. Rivera, M. Moukperian, D. Ashbrook, J. Mankoff, and S. E. Hudson, "Stretching the Bounds of 3D Printing with Embedded Textiles," in *Proceedings of the 2017 CHI Conference on Human Factors in Computing Systems*, Denver Colorado USA, 2017, pp. 497–508.

[4] igus® GmbH, *3D-Druck mit mehreren Filamenten: Extreme Lebensdauer und Belastbarkeit durch kombinierte Materialien.* [Online]. Available: https://www.igus.de/info/multimaterial-3d-druck (accessed: Dec. 30 2023).

[5] R. Freund, H. Watschke, J. Heubach, and T. Vietor, "Determination of Influencing Factors on Interface Strength of Additively Manufactured Multi-Material Parts by Material Extrusion," *Applied Sciences*, vol. 9, no. 9, p. 1782, 2019, doi: 10.3390/app9091782.

[6] A. Mühlbauer, *Multimaterial-Bauteile: Grundlage für die additive Fertigung von Kunststoffen.* [Online]. Available: https://www.additive-manufacturing-industry.de/news-fachartikel/multimaterial-bauteile.htm?thema=materialpruefung (accessed: Dec. 30 2023).

[7] Prusa Research, *Water soluble (BVOH/PVA)*. Material Guide. [Online]. Available: https://help.prusa3d.com/article/water-soluble-bvoh-pva_167012 (accessed: Dec. 30 2023).

[8] D. Chaidas, T. Spahiu, and J. Kechagias, "3D PRINTING ON TEXTILES USING THE FUSED FILAMENT FABRICATION: A KEY STUDY," in *Proceedings: Zbornik radova : V International Scientific Conference Contemporary Trends and Innovations in the Textile Industry, CT&ITI 2022 = V Međunarodna naučna konferencija Savremeni trendovi i inovacije u tekstilnoj industriji : Belgrade, 15-16th September 2022*, S. Urošević, Ed., Belgrade: Union of Engineers and Technicians of Serbia, 2022, pp. 56–62.

[9] M. Gorlachova and B. Mahltig, "3D-printing on textiles – an investigation on adhesion properties of the produced composite materials," *J Polym Res*, vol. 28, no. 6, 2021, doi: 10.1007/s10965-021-02567-1.

[10] M.-S. Özev and A. Ehrmann, "Sandwiching textiles with FDM Printing," *cdatp*, vol. 4, no. 1, pp. 88–94, 2023, doi: 10.25367/cdatp.2023.4.p88-94.
[11] Y.-Q. Xiao and C.-W. Kan, "Review on Development and Application of 3D-Printing Technology in Textile and Fashion Design," *Coatings*, vol. 12, no. 2, p. 267, 2022, doi: 10.3390/coatings12020267.
[12] Chromatic 3D Materials, *Chromatic 3D Materials Launches Rapid Custom Manufacturing Service for Common Rubber Parts with Uncommon Dimensions.* [Online]. Available: https://c3dmaterials.com/press-release-chromatic-launches-rapid-custom-manufacturing-service-for-common-rubber-parts-with-uncommon-dimensions (accessed: Dec. 30 2023).
[13] R. Pugliese, B. Beltrami, S. Regondi, and C. Lunetta, "Polymeric biomaterials for 3D printing in medicine: An overview," *Annals of 3D Printed Medicine*, vol. 2, p. 100011, 2021, doi: 10.1016/j.stlm.2021.100011.
[14] A. Liaskoni, R. D. Wildman, and C. J. Roberts, "3D printed polymeric drug-eluting implants," *International journal of pharmaceutics*, vol. 597, p. 120330, 2021, doi: 10.1016/j.ijpharm.2021.120330.
[15] *Advances in Healthcare and Protective Textiles*: Elsevier, 2023.
[16] *Regulation (EU) 2017/745 of the European Parliament and of the Council of 5 April 2017 on medical devices, amending Directive 2001/83/EC, Regulation (EC) No 178/2002 and Regulation (EC) No 1223/2009 and repealing Council Directives 90/385/EEC and 93/42/EEC: 2017/745*, 2023. Accessed: Dec. 30 2023. [Online]. Available: https://eur-lex.europa.eu/eli/reg/2017/745/2023-03-20
[17] S. Kreß, R. Schaller-Ammann, J. Feiel, J. Priedl, C. Kasper, and D. Egger, "3D Printing of Cell Culture Devices: Assessment and Prevention of the Cytotoxicity of Photopolymers for Stereolithography," *Materials (Basel, Switzerland)*, vol. 13, no. 13, 2020, doi: 10.3390/ma13133011.
[18] S. Berreta, O. Ghita, K. E. Evans, A. Anderson, and C. Newman, "Size, shape and flow of powders for use in Selective Laser Sintering (SLS)," in *ENGnetBASE 2015, High value manufacturing: Advanced research in virtual and rapid prototyping : proceedings of the 6th International Conference on Advanced Research and Rapid Prototyping, Leiria, Portugal, 1-5 October, 2013*, P. e. a. Bártolo, Ed., London, 2014, pp. 49–54.
[19] T. Spahiu, M. Al-Arabiyat, Y. Martens, A. Ehrmann, E. Piperi, and E. Shehi, "Adhesion of 3D printing polymers on textile fabrics for garment production," *IOP Conf. Ser.: Mater. Sci. Eng.*, vol. 459, pp. 12–65, 2018, doi: 10.1088/1757-899X/459/1/012065.
[20] B. Malengier, C. Hertleer, L. Cardon, and L. van Langenhove, "3D Printing on Textiles: Testing of Adhesion," ITMC2017 - International Conference on Intelligent Textiles and Mass Customisation, Gent, Oct. 2017. Accessed: Dec. 30 2023. [Online]. Available: https://www.researchgate.net/publication/320534534_3D_PRINTING_ON_TEXTILES_TESTING_OF_ADHESION
[21] M. Pelanconi, P. Colombo, and A. Ortona, "Additive manufacturing of silicon carbide by selective laser sintering of PA12 powders and polymer infiltration and pyrolysis," *Journal of the European Ceramic Society*, vol. 41, no. 10, pp. 5056–5065, 2021, doi: 10.1016/j.jeurceramsoc.2021.04.014.
[22] Shimadzu Europa GmbH, *Technische Daten AGS-X Serie.* [Online]. Available: https://www.shimadzu.de/technische-daten-ags-x-serie (accessed: Dec. 30 2023).
[23] J. Vlachopoulos and D. Strutt, "Rheology of Molten Polymers," in *Multilayer Flexible Packaging*: Elsevier, 2016, pp. 77–96.

[24] N. N., "Datasheet: PLA Extrafill," Jan. 2019. Accessed: Mar. 22 2024. [Online]. Available: fillamentum.com
[25] N. N., "Technical Data Sheet: ePA12," Nov. 2021. Accessed: Mar. 22 2024. [Online]. Available: https://esun3d.com/
[26] A. Biswas, J. L. Willet, S. H. Gordon, V. L. Finkenstadt, and H. N. Cheng, "Complexation and blending of starch, poly(acrylic acid), and poly(N-vinyl pyrrolidone)," *Carbohydrate Polymers*, vol. 65, no. 4, pp. 397–403, 2006, doi: 10.1016/j.carbpol.2006.01.035.